International Journal of Medical and Pharmaceutical Sciences
Open access peer-reviewed Journal
Volume 2, Issue 9, Page 602-620.
https://doi.org/10.5281/zenodo.23008145

Review Article

The Evolving Arsenal Against Naegleria Fowleri: From Empirical Poly-Chemotherapy to Target-Driven Repurposing Pipelines

Muhammed Danish Haneefa, Ashik T. N., Aparna E., Jisha Mohanan*

College of Pharmaceutical Sciences, Government Medical College, Kozhikode 673008, Kerala, India

Primary Amoebic Meningoencephalitis (PAM), caused by the thermophilic free-living amoeboflagellate *Naegleria fowleri*, is a hyperacute, devastating central nervous system infection characterized by rapid clinical progression and a fatal outcome exceeding 95% to 97% mortality globally. Current clinical management relies heavily on empirical poly-chemotherapy centered around intravenous amphotericin B, oral miltefosine, and azithromycin; however, these regimens are severely constrained by dose-limiting nephrotoxicity and hepatotoxicity, variable blood-brain barrier penetration, and therapeutic delays. This review provides a comprehensive synthesis of emerging small-molecule discovery pipelines, novel intracellular target landscapes, and advanced non-invasive therapeutic vectors against *N. fowleri*. In this review, we discuss key enzymatic bottlenecks, including glucokinase, enolase, protein farnesyltransferase, and sterol 14-α-demethylase (NfCYP51) and high-throughput phenotypic screening platforms that distinguish immediate-onset clearing agents (e.g., posaconazole, nitroxoline) from high-potency candidates with extended kinetic lag phases (e.g., azithromycin). We further assess potent synthetic chemicals (bis-benzimidazoles), natural product saponins, marine meroterpenoids and oxasqualenoid polyethers that exhibit stage-independent trophocidal and cysticidal clearance against *N. fowleri*. For the reason prevention is better than cure in many instances, we also describe rational multi-epitope mRNA vaccine designs, as well as novel transcribrial delivery systems, such as pressurized vaporized nasal inhalers and terpene-silver nanoconjugate fusions that exploit the naso-olfactory and glymphatic pathways to bypass systemic toxicity. Transitioning from historical empirical cocktails toward target-driven, rapid-acting, and locally delivered chemotypes offers a definitive paradigm shift to improve survival and clinical outcomes in PAM.

Keywords: *Naegleria fowleri,* Primary Amoebic Meningoencephalitis (PAM)**,** Drug Repurposing, High-Throughput Screening, Target-Driven Pharmacotherapy, Intranasal Nose-to-Brain Delivery, Anti-amoebic Agents.

INTRODUCTION

Naegleria fowleri is a ubiquitous, free-living eukaryotic ameboflagellate belonging to the class Heterolobosea and phylum Percolozoa. *N. fowleri* is the causative agent of Primary Amoebic Meningoencephalitis (PAM), a hyperacute, devastating, and typically fatal infection of the central nervous system (CNS).[1] It was historically categorized as a rare disease, however, recent epidemiological reports document an expanding global footprint, with increasing cases identified across countries such as India, Bangladesh, Taiwan, Turkey, Pakistan, Zambia and China.[2,3] Unfortunately, this dramatic shift in the epidemiological landscape of *N. fowleri*, has transitioned into an acute public health emergency. Even in India, this trend is particularly evident in Kerala, which faced an unprecedented escalation of CNS amoebic infections between 2024 and 2025.[4,5] Recognized clinically as an opportunistic, accidental neuroinvasive pathogen in humans, this single-celled organism transitions dynamically between three

distinct morphological life stages based directly on external environmental and nutritive stimuli:[6–9]

Table I: **The Tri-Phasic Life Stages of Naegleria fowleri**

Life Stage	Structural Dimensions and Diameter Range	Properties	Reference
Trophozoite	10 – 25 µm Amorphous ameboid shape	Active feeding form, drives cortical tissue trogocytosis	[6,9]
Flagellate	10 – 16 µm Pear-shaped biflagellated structure	Highly motile swimming vector, completely non-replicative	[6,9]
Mature Cyst	8 – 20 µm Spherical double-walled envelope	Resilient protective stage, completely refractory to drugs	[6,9]

1.1 Thermophilic Nature, Global Warming, and Clinical Emergency

Naegleria fowleri is a thermophilic microorganism, and shows optimal proliferation and survival rates at elevated temperatures up to 45°C–46°C. Since it cannot tolerate saltwater environments, its ecological niches are restricted to warm lakes, rivers, hot springs, stagnant public water storage tanks, and poorly chlorinated swimming pools. The progression of global warming and rising global surface water temperatures have expanded the geographic range of the pathogen into more areas previously deemed unhospitable, escalating the clinical urgency of monitoring this infection.[6,7,9] Infection is initiated when water contaminated with active trophozoites is forcefully introduced into the human nasal cavity during recreational swimming, diving, or nasal sinus irrigation. The amoebae rapidly utilize pseudopodia-driven locomotion to adhere to the nasal mucosa, bypassing host physical barriers. The trophozoites then penetrate through the olfactory neuroepithelium, destabilizing tight junction proteins (ZO-1, claudin-1, claudin-5, and occludin) and migrate passively along the paracellular spaces of primary olfactory sensory neurons.[6,9] Amoebae then migrate along non-myelinated olfactory nerve bundles *(fila olfactoria)* through the porous openings of the ethmoid cribriform plate (structurally more porous in children and young adults) to reach directly the olfactory bulb within the frontal cerebral cortex causing Primary Amoebic Meningoencephalitis (PAM).[10–12]

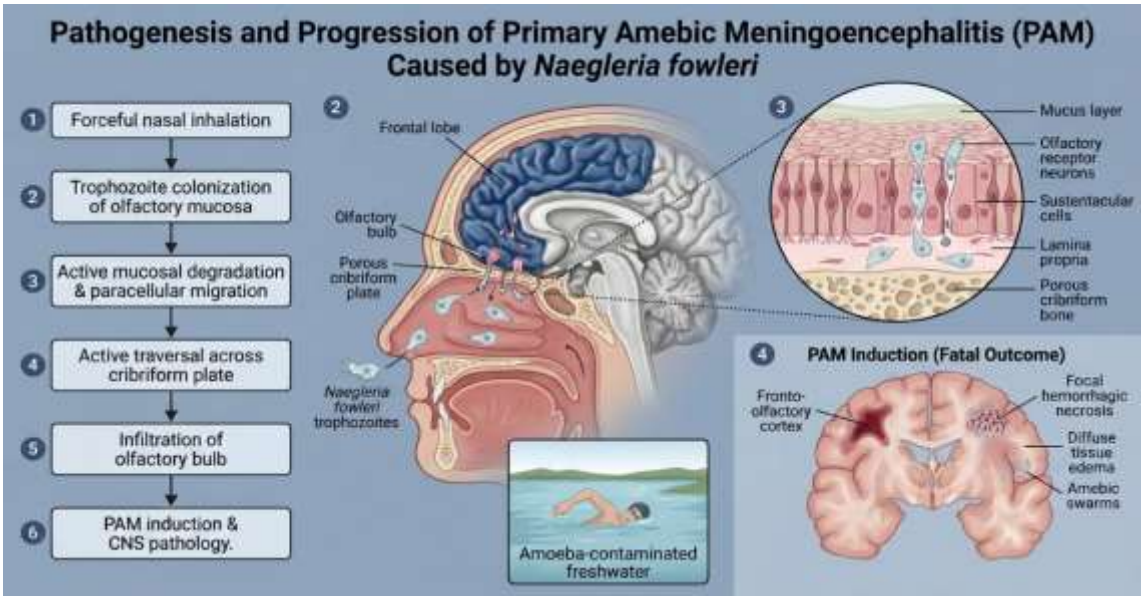

Figure 1: **Pathogenesis and progression of PAM caused by N.fowleri (Created in Scispace (https://scispace.com))**

The clinical presentation of PAM mimics acute bacterial or viral meningitis, leading to frequent misdiagnosis and significant delays in initiation of appropriate targeted treatment. Within 1 to 9 days post-exposure, patients manifest severe stage 1 symptoms, including intense bi-frontal headaches, acute fever, nausea, and projectile vomiting.[6,8,13] The disease quickly progresses to stage 2 complications, including stiff neck (nuchal rigidity), confusion, hallucinations, focal seizures, and extensive cerebral oedema. Ultimately, brain herniation drives the host into an irreversible coma stage, with death most probably occurring within 1 to 18 days from the initial onset of symptoms.[12,14,15]

1.2: Evolution of Empirical Poly-Chemotherapy Regimens

Due to the reason that PAM is an exceptionally rapid and fulminant infection with a global case fatality index exceeding 95% to 97%, the execution of controlled phase II or phase III clinical trials is not feasible. Current clinical therapies are entirely empirical, derived from retrospective case logs of a small number of global survivors.[6,12,13] The traditional therapeutic core relies on the broad-spectrum antifungal amphotericin B, administered both intravenously (1.5 mg/kg/day) and intrathecally (1.5 mg/day) to disrupt the ergosterol-rich membrane of the amoeba.[6,12,16] However, amphotericin B deoxycholate has a low rate of recovery due to its narrow therapeutic index and severe dose-limiting toxicities, most notably acute nephrotoxicity. To maximize chances of survival, current protocols use an aggressive multi-antimicrobial cocktail therapy designed to strike multiple cellular structures simultaneously by integrating the following agents:-[6,11,17]

Miltefosine: This alkylphosphocholine drug was initially developed as an antineoplastic candidate drug especially for breast cancer and later repurposed for visceral leishmaniasis. It is administered systematically to affect intracellular phospholipid metabolism and cell signalling networks in both trophozoite and cyst stages.[11,13,16]

Azithromycin: Included within primary interventions due to its ability to achieve high tissue concentrations within the brain parenchyma, azithromycin exhibits potent nanomolar growth inhibition *in vitro* and protects infected models *in vivo*[11,13,15,16]

Auxiliary Companion Adjuvants: Regimens incorporate the triazole fluconazole to inhibit sterol 14-alpha-demethylase pathways, the antibiotic rifampin to interfere with nucleic acid processing, and high-dose dexamethasone to control microglia-mediated neuroinflammation and decrease the cerebral oedema that drives fatal brain herniation.[6,12,13]

2: Clinical Paradigms and Case Efficacy Tracking

2.1: Epidemiological Surveillance and Diagnostic Bottlenecks

The striking clinical feature of PAM is the rapid progression of symptoms following exposure, which are misdiagnosed most often, leading to near-universal mortality. The patients present with non-specific signs such as severe frontal headache, acute fever, nausea, and projectile vomiting, are frequently misdiagnosed by clinicians as acute bacterial or viral meningitis.[6,11,13]

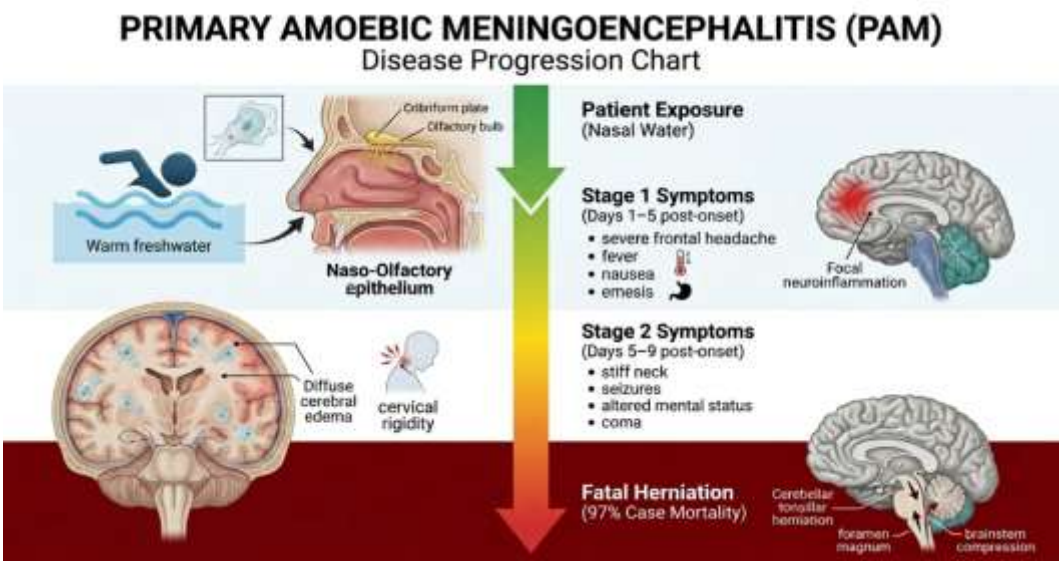

Figure 2: **Disease progression chart of PAM (Created in Scispace (https://scispace.com))**

The standard laboratory examination of cerebrospinal fluid (CSF) obtained via lumbar puncture of affected individuals displays elevated intracranial pressure (300 to 600 mm H_2O), purulent grey to yellowish-white discoloration, and high leukocyte counts. Identification of motile trophozoites on wet mounts or by Giemsa-Wright and trichrome stains is essential because more than three quarters of PAM cases are diagnosed post-mortem at autopsy[11,16] Advanced metagenomic next-generation sequencing (mNGS) of CSF has emerged as a powerful, non- assumptions-based tool capable of identifying low-abundance pathogens within 24 hours and has been successful in diagnosing rare clinical survivals that were missed by standard culture methods.[18]

2.2: Critical Efficacy Analysis of Frontline Therapeutics

Amphotericin B Permeability: Although amphotericin B remains the primary option for vegetative stage clearance, its systemic transport is blocked by the tight junctions of the BBB. Achieving minimum inhibitory concentrations in the central nervous system requires high intravenous doses that cause renal tubular acidosis and severe multi-organ toxicity.[11,18]

Miltefosine Tolerance and ADRs: Miltefosine is administered orally (50 mg 2-3 times per day for 28 days) based on its ability to cross the BBB and brain tissue accumulation. However, its clinical efficacy remains variable, and its extended use is associated with profound gastrointestinal side effects and potential ocular disorders[11,16]

The Fluconazole Efficacy Deficit: Fluconazole is often part of clinical combinations due to its low molecular weight and high free concentration within the CSF. However, systematic phenotypic screenings demonstrate that fluconazole is the least potent conazole against *N. fowleri*, resolving extremely weak in vitro activity ($EC_{50} = 13.9\ \mu$M to $> 100\ \mu$M) and failing to extend survival when tested in monotherapy in vivo.[11,16]

3: The Target Driven Repurposing Pipelines against *N. fowleri*

Recent drug discovery efforts have focused on target-driven repurposing pipelines against *N. fowleri* to overcome the clinical failures, high toxicity and limited efficacy of conventional treatment regimens.[13]These approaches exploit fundamental parasite vulnerabilities to validate fast-acting leads with defined, verifiable mechanisms of action.[11,13,16]

3.1: Intracellular Enzyme Targets and Drug Susceptibility

3.1.1: Glycolytic and Kinase Target Validation

Phenotypic screening and transcriptome profiling have chemically validated specific intracellular multi-enzyme pathways in *Naegleria fowleri* that are

completely absent or structurally distinct from human hosts. The energy metabolism of amoeba relies on specialized glycolytic enzymes, including glucokinase (NfGK) and enolase, to regulate carbohydrate catabolism and ATP synthesis. Targeting enolase with small-molecule inhibitors disrupts this glycolytic cascade, resulting in cellular energy depletion and growth arrest in vitro.[11,13] Parallel screening of heterocyclic small-molecule libraries has identified synthetic imidazo[2,1-b] thiazole derivatives as potent anti-protozoal candidates. Originally engineered to bind to the intracellular catalytic domains of mammalian RAF kinases to treat malignant melanoma, these cell-permeable molecules readily penetrate the protozoal cell membrane. Exposing active trophozoites to these imidazothiazoles induces statistically significant ($p \leq 0.05$) amoebicidal actions, with advanced analogs (compounds 1h and 1j) driving pathogen survival down to 15.14% and 17.45%, respectively, within a standard 24-hour incubation window[18]

3.1.2: Downstream Blockades of the Mevalonate and Farnesylation Axis

The mevalonate pathway is a critical drug target in *N. fowleri.* It controls the de novo synthesis of sterol intermediates necessary for cell wall structure as well as crucial non-sterol lipids, such as farnesyl pyrophosphate (FPP). At the end of this branch is the enzyme protein farnesyltransferase (FT) which catalyses the direct transfer of the hydrophobic 15-carbon farnesyl group from FPP onto conserved cysteine residues located within a classic CaaX motif present on target regulatory proteins. This prenylation loop is an absolute prerequisite for membrane docking, directing small Ras-like GTPases and signalling molecules to associate with and organize within the plasma membrane bilayer.[13,15]

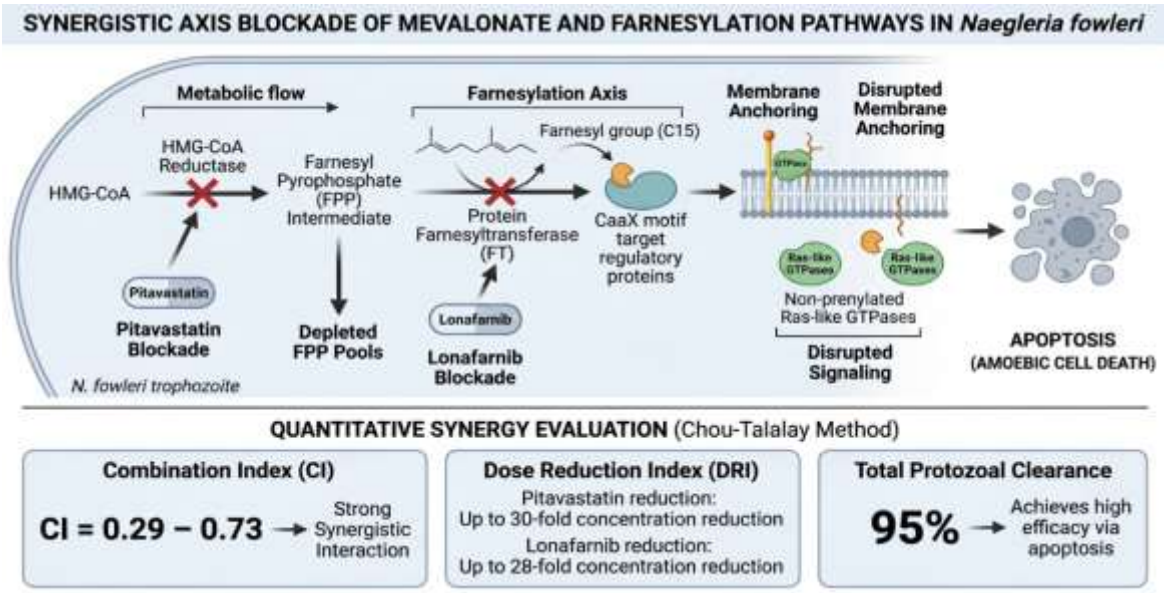

Figure 3: **Synergistic drug therapy for N.fowleri (Created in Scispace (https://Scispace.com))**

The clinically advanced farnesyltransferase inhibitor lonafarnib binds selectively the FT complex of the pathogen, disrupting lipid anchoring loops. Susceptibility testing against a range of international strains revealed that lonafarnib inhibits vegetative growth with an EC_{50} of 1.5 µM against the European KUL strain and 2.5 µM against the Australian V1005 isolate[15] Moreover, the combination of lonafarnib with pitavastatin, a potent HMG-CoA reductase inhibitor, simultaneously targets two distinct bottlenecks in the mevalonate pathway. In vitro quantitative assessment using the Chou-Talalay method revealed strong synergistic interactions (CI = 0.29 to 0.73), resulting in a significant dose reduction index (DRI) with up to a 30-fold reduction in statin concentration and a 28-fold reduction for the farnesyltransferase inhibitor while achieving 95% total protozoal clearance.[15]

3.2: Host-Parasite Defensome Interactivity and Innate Immunity

3.2.1: Humoral Mucosal Barriers and Proteolytic Neutralization Matrix

The respiratory mucosa of the upper airway is the first line of defense against inhaled amoeboflagellates. The Bowman's glands secrete a thick layer of mucus that forms a physical barrier preventing the parasite from directly attaching to the ciliated microvilli. The mucus also contains high concentrations of innate antimicrobial proteins including mucins, lactoferrin and lysozyme. To investigate these protective networks, individual and combined administrations of bovine milk lactoferrin (bLf) and chicken egg lysozyme (cLz) were carried out against active *N. fowleri* trophozoites.[11,19] Axenic whole-cell survival profiling reveals a significant biological paradox: the pathogen is completely resistant to the direct microbicidal or microbistatic actions of these innate proteins. In trypan blue exclusion assays, high doses (500 µM bLf and 20 µM cLz) caused no reduction in parasite viability, which remained stable at 95% across all 24-hour time points. High-resolution transmission electron microscopy (TEM) confirms that the amoebae respond to the dual bLf-cLz combination by undergoing temporary extensive vacuolation, developing autophagic vacuoles filled with dense debris, before completely recovering normal amoeboid morphology and normal nuclear architecture within 24 hours.[20] To characterize the mechanism behind this resistance, gelatin-zymography was deployed to analyze the protease expression profile within the parasite's conditioned medium (CM) secretome. Invading trophozoites actively secrete potent extracellular cysteine proteases that resolve clear lytic bands at 150 and 73 kDa. These secreted cysteine protease enzymes cleave and neutralize host lactoferrin and immune complexes.[20]

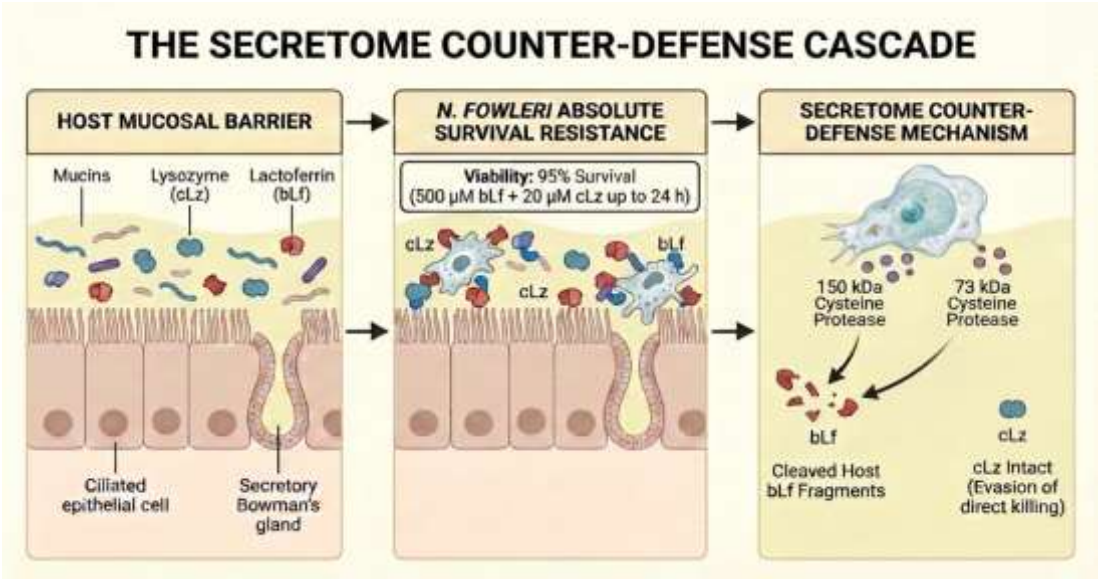

Figure 4: Secretome counter defense cascade of N.fowleri against host innate mucosal immunity (Created in Scispace (https://Scispace.com))

Pre-incubation of the CM secretome with specific cysteine protease inhibitors (such as E-64 at 10 µM or pHMB) completely inhibits lactoferrin degradation, confirming that *N. fowleri* uses specialized cysteine proteases as a primary counter-defense mechanism against host innate defensomes.[20] Despite the complete lack of direct amebicidal action (leaving total parasite viability unchanged), co-incubating the parasite with the dual bLf-cLz combination acts as an anti-virulence barrier. By occupying and neutralizing the parasite's secreted extracellular proteases, the bLf-cLz combination prevents these enzymes from attacking host tissues, thereby protecting human epithelial monolayers from amoebic destruction by up to 80%.[20]

3.2.2: Humoral Antibody Protection and Cytokine Immunopathology

Passive transfer challenges conducted in syngeneic animal models demonstrate that humoral immunity plays a critical role in preventing nasal mucosal invasion. Naive recipient mice exposed to a lethal

intranasal challenge ($25\,\mu$L of active suspension containing 2×10^6 organisms/mL) are successfully rescued from PAM following the intravenous transfer of hyper-immune serum or its purified IgG fraction harvested from donors immunized with cell-free amoeba culture fluid (ACF).[21] ELISA mapping and indirect immunofluorescence assays confirm that these protective antibodies bind specifically to surface-exposed epitopes on the protozoal plasmalemma, causing agglutination and blocking neuro-mucosal adhesion. In contrast, transfer of viable immune spleen cells fails to protect recipients unless the challenge is delayed by 10 days, a lag phase required for the transferred cells to synthesize and release anti-naegleria antibodies *in vivo*.[21]

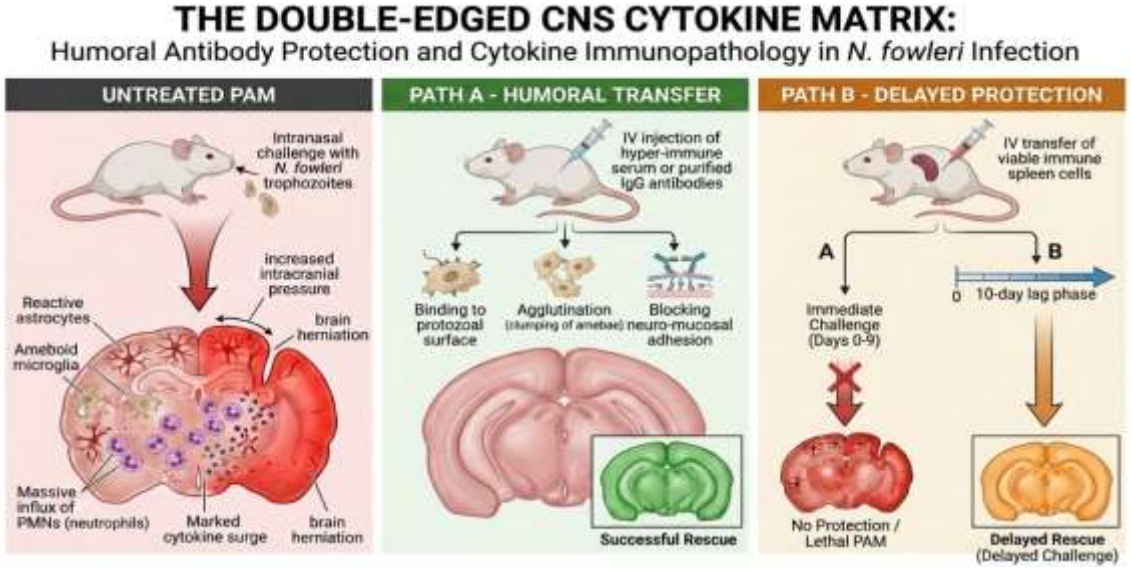

Figure 5: **Mechanism of pathology and humoral protection of PAM (Created in Scispace (https://Scispace.com))**

Once trophozoites successfully cross the cribriform plate and breach the CNS, resident microglia and astrocytes activate the NLRP3 inflammasome and MAPK signalling pathways. This results in a hyperacute pro-inflammatory cytokine storm, leading to transcription and release of IL-1α, IL-1β, IL-6 and TNF-α. This intense local cytokine environment is required for an anti-amoebic purpose by licensing recruited blood-borne neutrophils to maximize respiratory bursts and execute extracellular trap (Net) formation.[19] However, this unregulated inflammatory response results in severe immunopathology in the limited space of the intracranial cavity. Massive influx of polymorphonuclear leukocytes (PMNs) and cytokine-driven vascular permeability result in extensive vasogenic oedema, intracranial hypertension and brain herniation confirming that the host immune response contributes directly to fatal PAM outcomes.[19]

3.2.3: Clinical Adjunctive Therapeutics: Dexamethasone and Hypothermia

In order to alleviate this self-destructive inflammatory cascade, corticosteroid dexamethasone is currently incorporated as a standard component of multi-drug regimens against *N. fowleri*. Dexamethasone suppresses cytokine transcription in microglia, stabilizes compromised tight junctions in the blood brain barrier, reduces spikes in intracranial pressure, and protects adjacent cortical tissues from collateral immune damage.[12,13,18]

3.2.3.1: Neuroprotective Mechanisms of Induced Hypothermia in Paediatric PAM Patients

The rapid, destructive progression of Primary Amoebic Meningoencephalitis necessitates the use of adjunctive multi-targeted approaches to preserve the host brain tissue until anti-microbial therapy takes effect.[12] Induced therapeutic hypothermia is highly validated clinical intervention, during which a patient's core body temperature is systematically

reduced to and maintained within a targeted cooling window of 32°C to 34°C for an extended multi-day duration.[12] Induced hypothermia provides multi-targeted protection through three distinct physiological mechanisms:-[12,22]

Direct Pathogen Growth Suppression: *N. fowleri* is a highly thermophilic organism that exhibits optimal proliferation and virulence kinetics at elevated temperatures ranging from 37°C to 45°C. Lowering the local parenchymal environment to 32°C severely depresses the amoeba's metabolic kinetics, arresting cellular replication, impairing flagellar transition, and retarding the secretion of tissue-destructive cysteine proteases like cathepsin B.[12,22]

Vascular Stabilization and Intracranial Pressure (ICP) Regulation: Acute meningitis triggers severe vasogenic oedema, disrupting endothelial tight junctions and leading to fatal brain herniation spikes. Controlled cooling by induced hypothermia substantially lowers local metabolic demand, decreases cerebral blood volume, blocks free-radical accumulation and stabilizes blood-brain barrier junctions. This effectively alleviates ICP and prevents tissue compression.[12]

Attenuation of Cytopathic Neuroinflammation: By downregulating the nuclear factor-kappa B (NF-κB) signalling in resident microglia, therapeutic hypothermia significantly reduces host-mediated immune damage and halts the release of destructive pro-inflammatory cytokines (IL-6, TNF-α). This inhibition ultimately limits the aggressive "neutrophil storm" that drives cortical necrosis.[12]

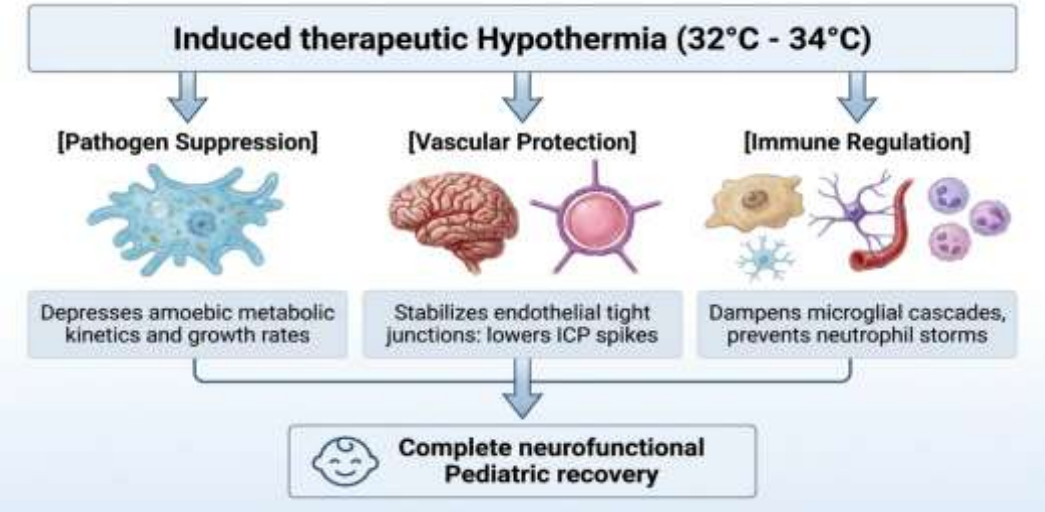

Figure 6: Neuroprotective mechanisms of induced hypothermia in paediatric PAM patients (Created in Scispace (https://scispace.com))

Systematic reviews across 55 documented paediatric PAM patients confirm that controlled therapeutic hypothermia provides significant neuroprotective benefits.[12,13]Statistical metadata analysis confirms that while the baseline paediatric PAM mortality rate remains high at 85.5% (47/55), treating patients with induced hypothermia combined with aggressive multi-drug regimens (including miltefosine) significantly improves survival outcomes, often leading to complete neurological recovery without impairments, validating hypothermia as an essential clinical protocol.[12]

3.3: High-Throughput Screening Methodologies and Library Repurposing

3.3.1: Microtiter Platform Optimization and High-Throughput Standardization

The identification of reproducible, high potency anti-amoebic leads has required a critical methodological transition: moving away from traditional, low-throughput visual cell counting techniques toward automated whole-cell phenotypic screening platforms. Historically, screening of candidate drugs required large culture volumes (> 10 mL per flask) and long multi-day observation periods. These legacy

methods were resource-intensive, consumed large volumes of expensive reagents, and introduced a large inter-operator counting bias.[13,16,17] To standardize modern drug discovery pipelines, researchers established and validated automated high-throughput assays using flat-bottomed 96-well and 384-well microtiter plates over a compressed 72-hour drug-exposure window.[17]

Table II: **The 72-Hour Automated Whole-Cell Screening Standard**[17]

Assay Type	96-Well Seeding Density	384-Well Seeding Density
Fluorometric alamarBlue Assay	100,000 cells/well	3,000 cells/well
Luminescent CellTiter-Glo Assay	4,000 cells/well	3,000 cells/well

Carefully standardizing cell-seeding parameters across these microplate wells improved assay precision, yielding high signal-to-noise ratios with a Z' factor ranging from 0.51 to 0.95. This metrics confirm the method's reliability for large-scale library screening.[13,17]

3.3.2: Large-Scale Repurposing Inventories: ReFRAME and Pathogen Box Mining

Using these optimized microtiter systems, researchers conducted the first large-scale chemical library screen against pathogenic *N. fowleri*. They screened the Calibr ReFRAME library (a collection of approximately 12,000 clinically evaluated small molecules) alongside the Medicines for Malaria Venture (MMV Pathogen Box), identifying several potent repurposing hits.[13,16]

While earlier studies focused on sterol 14-demethylase (NfCYP51) inhibitors like posaconazole ($IC_{50} = 240$--860 nM), as potent anti-amoebic leads, this revealed additional targets, including MetAP2, heat shock proteins, and protein kinase pathways.[13,16] Furthermore, cross-screening these active leads against multiple diverse geographical isolates including cerebrospinal fluid (CSF) derived clinical lines-V067, V596, V414, and V413 showed no statistically significant difference in calculated IC_{50} values ($p > 0.05$). This uniform activity indicates that the candidate drugs act on essential targets conserved across global strains.[13,16]

Table III: **High-Potency and Rapid-Acting Candidates Identified from the ReFRAME Library Against Naegleria fowleri**[13]

Candidate Compound	Class / Indication	In Vitro Potency (qAC_{50})	Rate of Action ($1\times IC_{50}$)	Proposed Mechanism of Action
Beloranib hemioxalate	Antineoplastic	0.02 μM ($\pm$0.06)	8 hours	Methionine Aminopeptidase-2 (MetAP2) inhibitor
Oligomycin B	Antibacterial	0.06 μM ($\pm$0.03)	No effect	ATP synthase inhibitor
Fimepinostat	Antineoplastic	0.13 μM ($\pm$0.04)	23 hours	Histone deacetylase (HDAC) inhibitor
Fumagillin	Antineoplastic	0.15 μM ($\pm$0.20)	10 hours	Methionine Aminopeptidase-2 (MetAP2) inhibitor
Staurosporine	Antibacterial	0.21 μM ($\pm$0.04)	34 hours	Protein kinase C inhibitor
Terbinafine HCl	Antifungal	0.23 μM ($\pm$0.17)	36 hours	Squalene monoxygenase inhibitor
AGM-1470	Antineoplastic	0.29 μM ($\pm$0.11)	29 hours	Methionine Aminopeptidase-2 (MetAP2) inhibitor
Azithromycin	Antibacterial	0.29 μM ($\pm$0.06)	26 hours	23S-rRNA of 50S ribosomal subunit inhibitor
Latrunculin B	Antineoplastic	0.33 μM ($\pm$0.06)	No effect	Disrupts actin cytoskeleton
Bardoxolone	Antineoplastic	0.34 μM ($\pm$0.03)	8 hours	NF-kB pathway inhibitor
Bardoxolone methyl A	Antineoplastic	0.36 μM ($\pm$0.011)	8 hours	NF-kB pathway inhibitor
Nitracrine 2HCl	Antineoplastic	0.42 μM ($\pm$0.02)	24 hours	Nucleoside inhibitor

Valnemulin	Antibacterial	0.42 μM ($\pm$0.22)	No effect	50S ribosomal subunit inhibitor
JNJ-16241199	Antineoplastic	0.52 μM ($\pm$0.10)	36 hours	Histone deacetylase (HDAC) inhibitor
Quisinostat	Antineoplastic	0.75 μM ($\pm$0.12)	16 hours	Histone deacetylase (HDAC) inhibitor
Erythromycin	Antibacterial	0.77 μM ($\pm$0.19)	ND	23S-rRNA of 50S ribosomal subunit inhibitor
BC-3205	Antibacterial	0.83 μM ($\pm$0.11)	17 hours	23S-rRNA of 50S ribosomal subunit inhibitor
Tractinostat	Antineoplastic	0.97 μM ($\pm$0.11)	26 hours	Histone deacetylase (HDAC) inhibitor
Halofuginone	Antifibrotic	1.49 μM ($\pm$0.02)	2 hours	Prolyl tRNA synthetase inhibitor
NVP-HSP990	Antineoplastic	2.49 μM ($\pm$0.17)	10 hours	HSP90 inhibitor
BPH-942	Antimalarial	5.10 μM ($\pm$0.09)	11 hours	Farnesyl diphosphate synthase inhibitor

Abbreviations: qAC_{50}-concentration for half-maximal activity; h-hours; ND-not determined.

As detailed in Table *III* (encompassing 21 representative lead compounds), the top hit beloranib hemioxalate demonstared high potency of 20 nM ($qAC_{50} = 0.02\ \mu$M) with an onset of action within 8 hours. In addition, the selected candidates showed rapid parasite clearance within hours of exposure, notably halofuginone ($qAC_{50} = 1.49\ \mu$M), which suppressed metabolic activity within 2 hours. These rapid-acting leads have a distinct pharmacodynamic advantage over conventional agents such as azithromycin, which exhibits a 30-hour lag phase before suppressing parasite growth.[13]

3.3.3: Kill Kinetics and Onset Speed: Evaluating Real-Time Amoebicidal Action

Primary amoebic meningoencephalitis (PAM) progresses rapidly, with a median interval of 5 days from hospitalization to brain death; thus, drug candidates require rapid onset kinetics. Conventional endpoint assays cannot capture cell death rates during the initial hours of exposure. To address this limitation, a real-time kinetic assay using a cell-compatible luminescent substrate (RealTime-Glo) was validated for continuous monitoring of metabolic viability.[16]

3.3.3.1: The Kinetic Readout Paradox in Azithromycin versus Posaconazole

Table IV: **Real-time kinetic profiles of Azithromycin and Posaconazole:**[13,16]

Compound	Kinetic Phenotype	Temporal Profile	Primary Mechanistic Rationale
Azithromycin	Lag Phase Phenotype	Delayed (~30-hours)	Requires intracellular drug accumulation prior to inhibiting ribosomal mRNA translation and peptide elongation.
Posaconazole	Clearance Influx Phenotype	Rapid (~12-Hour)	Rapid disruption of the ergosterol pathway by Inhibhit sterol 14-demethylase (NfCYP51), directly disrupting ergosterol synthesis and destabilizing the cell membrane.

The Macrolide Lag Phase: While azithromycin exhibits nanomolar potency in standard 72-hour endpoint assays, real-time monitoring reveals a 30-hour lag phase prior to the inhibition of amoebic growth. This delayed onset is consistent with its mechanism to gradually disrupt ribosomal peptide elongation rather than to abruptly change membrane integrity.[13,16]

Rapid Clearing Agents: In contrast, posaconazole and nitroxoline display swift onset kinetics, markedly reducing parasite metabolic activity within the first 12 hours of exposure.[6,16]

This kinetic difference presents an important clinical protocol: multi-drug cocktails should begin with fast-acting clearing agents that immediately arrest tissue

trogocytosis, followed by slower macrolides for complete and sustained parasite clearance.[16]

3.4: Synthetic Small-Molecule Scaffolds and Lead Optimization

3.4.1: Heterocyclic compounds and Diamidine Derivatives

Screening small-molecule libraries across six structural classes defined the chemical features required for the optimization of direct anti-protozoal activity with minimal toxicity to mammalian cells. From these screens, two bis-benzimidazole series emerged as primary leads: bis-benzimidazole monoamidines (Type I) and bis-benzimidazole diamidines (Type II).[13,16] Structure-activity relationship (SAR) analysis shows that minor modifications of the terminal aromatic rings alter the calculated IC_{50} from micromolar levels to narrow nanomolar limits:[13]

Table V: Structure–Activity Relationship (SAR) and Selectivity Indices of Heterocyclic Lead Candidates Against Naegleria fowleri[13]

Compound Class	Structural Architecture	Anti-*N. fowleri* Potency (IC_{50})	Cytotoxicity (IC_{50} J774)	Selectivity Index (SI)	Key SAR Finding
DB173	Type I Bis-benzimidazole Monoamidine	177 nM	7.9 μM	44.6	Optimal monocationic lead; peak potencies and macrophage selectivity.
DB1766	Type II Bis-benzimidazole Diamidine	430 nM	> 10 μM	> 23.2	Optimal dicationic lead; acutely curved geometry enhances clearance.
Furamidine Analogs	Furamidine Core Derivatives	5.0 to > 10 μM	—	Low	Core modification results in major loss of anti-amoebic activity.
Diarylbenzimidazoles & Diarylindoles	Diaryl Diamidines	5.0 to > 10 μM	—	Low	Demonstrates efficacy is strictly specific to bis-benzimidazole framework.

Abbreviations: IC_{50}, half-maximal inhibitory concentration; J774, murine macrophage cell line; SI, Selectivity Index (IC_{50} [J774]/IC_{50} [N. fowleri] Parallel screenings of related structural classes including furamidine analogues, diarylbenzimidazole diamidines, and diarylindole diamidines exhibited poor potency ($IC_{50} = 10$ μM to > 84 μM).[13] This loss of activity highlights that anti-amoebic activity requires the bis-benzimidazole core, establishing a key SAR baseline for future compound design.[13]

3.5: Natural Product Scaffolds and Marine Meroterpenoids

3.5.1: Terrestrial Phytochemical Metabolites and Pentacyclic Saponins

Exploring natural plant-derived secondary metabolites provides a huge resource of bioactive molecules with unique mechanisms of action. Chromatographic separation of lipophilic extracts prepared from the leaves of *Salvia triloba* and the aerial parts of *Rinorea yaundensis* led to the isolation of multiple pure active metabolites. Exposing axenic *N. fowleri* trophozoites to these compounds over a 24-hour incubation window identified three pentacyclic triterpenoid saponins that were found to achieve significant, concentration dependent clearance:[23]

Table VI: In Vitro Amoebicidal Activity of Plant-Derived Saponins Against Naegleria fowleri (24 h Exposure)

Active Metabolite	Plant Origin	Trophozoite Viability (%)	MIC	Reference
Betulin Core Matrix	Salvia triloba / Rinorea yaundensis	14.82%	77.00 µg/mL	[23]
Betulinic Acid Scaffold	*Salvia triloba* / *Rinorea yaundensis*	28.19%	34.39 μg/mL	[23]
Ursolic Acid Core	*Salvia triloba* / *Rinorea yaundensis*	49.30%	74.67 μg/mL	[23]

Among these, the Betulin core scaffold exhibited the highest baseline potency, reducing trophozoite survival to 14.82%.[23] Cytotoxicity evaluations on HeLa monolayers confirmed broad mammalian safety for these pentacyclic triterpenoids, with baseline cytotoxicity below 20%, except for betulinic acid, which exhibited mild cytotoxicity (37% cell compromise).[23] Importantly, a 2-hour pre-treatment of N. fowleri trophozoites significantly reduced host tissue damage with betulin, betulinic acid, and ursolic acid restricting tissue destruction to 24%, 28%, and 49% (preserving 51% viability), respectively.[23] Parallel susceptibility mapping of West African native terrestrial flora confirms that the ethanolic extract of *Xylopia aethiopica* fruits also exhibits high direct anti-protozoal action, with a calculated IC_{50} value of 18.5 μg/mL against active trophozoites. The SAR studies attributed this potency to the presence of abundant lipophilic diterpenes of the kaurane class, which target amoebic membrane lipids and disrupt the transmembrane potential to trigger apoptotic cell death.[24]

3.5.2: Marine Meroterpenoids from *Gongolaria abies-marina*

The marine derived meroterpenoids have gained increasing attention as structural scaffolds for anti-protozoal drug discovery. Bio-guided fractionation of lipophilic extracts prepared from the brown marine alga *Gongolaria abies-marina* (collected from the Canary Islands) led to the isolation of six pure meroterpenoid molecules: gongolarone B, 6Z-1'-methoxyamentadione, 1'-methoxyamentadione, gongolarone A, gongolarone C, and cystomexicone B.[25] In vitro viability assays using colorimetric alamarBlue parameters demonstrate that three of these isolated algal meroterpenoids induce rapid, low-micromolar growth inhibition, outperforming frontline chemical standards:[25]

Table VII: In Vitro Anti-Amoebic Activity of Meroterpenoids Isolated from Gongolaria abies-marina Against Naegleria fowleri Strains

Active Meroterpenoid	*N. fowleri* Strain	IC_{50} Value	Reference
6Z-1'-Methoxyamentadione	ATCC 30215	13.27 ± 0.96 μM	[25]
1'-Methoxyamentadione	ATCC 30215	16.51 ± 0.96 μM	[25]
Gongolarone B	ATCC 30215	18.85 ± 0.94 μM	[25]
	ATCC 30808	21.92 ± 1.60 μM	

Cytotoxicity evaluation in J774A.1 murine macrophages demonstrated low toxicity for cystomexicone B ($CC_{50} > 500$ μM), yielding a selectivity index greater than 8.5.[25] Fluorometric assays showed that these meroterpenoids induce a mitochondria-dependent, apoptosis-like cell death pathway in *N. fowleri*. Compound exposure resulted in chromatin condensation (Hoechst 33342 staining), plasma membrane permeabilization (SYTOX Green assay), and loss of inner mitochondrial membrane potential, which ultimately depleted cellular ATP.[25]

3.5.3: Marine Oxasqualenoid Polyethers and the C-18 Ketone Inversion Paradox

Squalene-derived polyether metabolites isolated from the red marine alga *Laurencia viridis* exhibit broad-spectrum anti-parasitic activity against *N. fowleri* trophozoites. Standardized whole-cell phenotypic screenings evaluating six pure isolated oxasqualenoid structures identified yucatecone and the semisynthetic analog 18-ketodehydrotyrsiferol as high-potency candidates.[26] Structure-activity relationship analysis reveals an electronic paradox governing this chemical family. While the native metabolite dehydrotyrsiferol shows no activity against both *N. fowleri* strains (IC_{50} = N/A), oxidation of its C-18 hydroxyl group to a carbonyl group yields 18-ketodehydrotyrsiferol, converting an inactive compound into a potent anti-amoebic lead.[26] Dose-response curve evaluation confirms that this C-18 ketone structure achieves potent growth inhibition, outperforming frontline chemical controls:[26]

Table VIII: Anti-amoebic activity and cytotoxicity metrics of oxasqualenoid derivatives against Naegleria fowleri

Active Candidate	*N. fowleri Strain*	IC_{50}	Reference
18-Ketodehydrotyrsiferol	ATCC 30215 (Clinical)	$12.70 \pm 2.64\ \mu$M	[26]
	ATCC 30808	$15.33 \pm 2.82\ \mu$M	
Yucatecone	ATCC 30215 (Clinical)	$16.25 \pm 1.23\ \mu$M	[26]

Its structural derivative, yucatecone, reaches two major therapeutic milestones: it penetrates the protective, double-walled cyst barrier of *N. fowleri* and triggers mitochondria-dependent, non-lytic apoptosis. By permeabilizing the parasite membrane without causing rapid cell lysis, yucatecone minimizes the release of intracellular contents, avoiding severe host neuroinflammation.[26] Moreover, Density Functional Theory (DFT) modelling confirms that the C-18 ketone significantly increases the molecule's dipole moment (from 3.020 D to 7.909 D), optimizing its lipophilicity for passive traversal across the Blood–Brain Barrier.[26]

3.6: Next-Generation Rational Vaccinology & Preventative Horizons

3.6.1: Multi-Epitope mRNA Vaccine Architecture

While small-molecule chemotherapeutic discovery remains critical, the development of effective immunoprotective agents would be a major milestone in the attainment of long-term sterilizing immunity against Primary Amoebic Meningoencephalitis. To bridge this technological gap, modern immune-informatics and reverse vaccinology approaches were used to design a highly immunogenic, multi-epitope mRNA-based vaccine against conserved, surface-exposed pathogenic proteins of *Naegleria fowleri* mined directly from the UniProt database.[27] By screening virulence-associated outer membrane antigens, researchers identified 30 highly antigenic, non-allergenic B-cell, cytotoxic T-lymphocyte (CTL), and helper T-lymphocyte (HTL) epitopes.[27] The multi-epitope vaccine construct was designed to maximize the recruitment of host immune responses by systematically linking the prioritized epitope sequences with specific structural spacer components and secretion enhancers. The highly immunogenic RpfE adjuvant (a resuscitation-promoting factor fragment) was added at the amino-terminus through a rigid EAAAK linker to activate toll-like receptor 4 (TLR-4) signalling pathways on host antigen-presenting cells.[27] The individual CTL and HTL epitope segments were subsequently joined using flexible linkers, preventing the formation of neo-epitopes and optimizing proteasomal processing and MHC class I/II presentation. Linear B-cell epitopes were fused to the carboxy-terminus with a highly flexible bi-peptide spacer to guarantee maximum surface exposure for antibody recognition.[27]

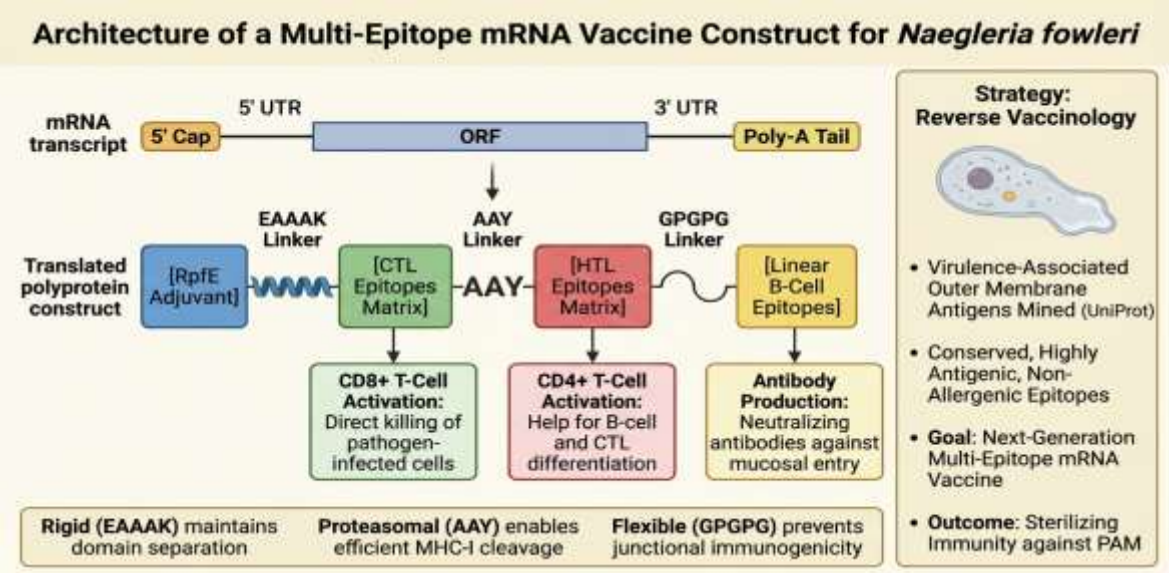

Figure 7: Architecture of a multi-Epitope mRNA vaccine against N.fowleri (Created in (https://Scispace.com))

The safety and stability of the final vaccine construct was confirmed by thorough physicochemical characterization and structural modelling:[27]

Table IX: Physicochemical characterization and structural modelling of vaccine construct

Property Category	Parameter/ Tool	Values	Interpretation	Reference
Antigenicity and Allergenicity	VaxiJen Score	0.80	Exceptional baseline immunogenic potential	[27]
	Allergenicity Mapping	Non-allergenic	Safe for mammalian administration	
Physicochemical Telemetry	GRAVY Index	-0.394	Favourable hydrophilic/ hydropathy profile	[27]
	Instability Index	38.99	Classified as a highly stable protein (< 40)	
Structural Validation	Ramachandran Plot	93.8%	Residues locked within highly favoured core regions	[27]

Dynamic immunological simulations modelling a three-dose schedule (administered at 4-week intervals) predict a strong, multi-clonal protective response. The vaccine triggers a rapid increase in active B-cell populations and high levels of immunoglobulins (IgGM and IgG1+IgG2), and with a corresponding increase in helper T-cell density and elevated cytotoxic interferon-gamma (IFN-γ) and Interleukin-2 (IL-2) release profiles.[27] For advanced formulation design, encapsulation of this optimized multi-epitope mRNA sequence within mucoadhesive lipid nanoparticles (LNPs) or chitosan-functionalized nanocarriers is a highly viable strategy to achieve direct mucosal immune activation within the nasal cavity, thereby generating a protective antibody barrier at the primary site of pathogen entry.[21,27]

3.6.2: Mucosal Adjuvants and Proteinaceous Immunogens: The Cry1Ac Protoxin Benchmark

While in silico multi-epitope mRNA construct design represents the modern vaccinology frontier[27], in vivo proof-of-concept for complete mucosal protection was established using non-toxic proteinaceous adjuvants[28]. Intranasal co-administration of the *Bacillus thuringiensis* Cry1Ac protoxin with *N.*

fowleri amoebal lysates achieved 100% survival in BALB/c mouse models subjected to a lethal intranasal challenge (5×10^4 live trophozoites)[28]. Notably, intranasal administration of Cry1Ac alone showed a 60% survival rate, highlighting its capacity to directly stimulate local innate mucosal defenses[28]. Immunological tracking revealed that survival did not correlate with systemic serum antibody titers, but rather with a rapid, transient surge in nasopharyngeal and tracheopulmonary IgA (peaking 1 to 3 days post-exposure) paired with sustained local mucosal IgG levels[28]. As a low-cost, non-toxic mucosal adjuvant, Cry1Ac offers a validated proteinaceous platform that could be co-formulated into next-generation intranasal subunit or mRNA-nanocarrier vaccines to halt trophozoite invasion at the primary nasopharyngeal boundary[27,28].

3.7: Advanced Delivery Vector Frontiers: Pressurized Inhalers & Hybrid Nanoconjugates

3.7.1: Vaporized Transcribrial Inhalers and Glymphatic Transport Routes

The management of acute primary amoebic meningoencephalitis requires the use of non-invasive drug delivery systems that can rapidly achieve minimum inhibitory concentrations directly within the central nervous system. While standard clinical protocols rely on aggressive, large-dose intravenous infusions such as Amphotericin B (5–10 mg/kg/day), this systemic route faces severe transport limitations due to the tight junction selectivities of the blood-brain barrier. This necessitates a transition toward localized intranasal delivery systems which circumvent this limitation by utilizing direct naso-olfactory neural pathways into the CNS.[10,20] The delivery of vapourised anti-amoebic drug combinations using pressurized nasal inhalers is an innovative approach to improve transport kinetics. Therapeutic delivery in a gaseous or vapourised form exploits the host glymphatic system by using the perivascular fluid channels associated with trigeminal and olfactory nerve pathways to rapidly distribute molecules throughout the cerebral cortex. This non-invasive route of delivery completely bypasses the systemic circulation, avoiding hepatic first-pass metabolism and thereby eliminating the dose-limiting nephrotoxicity and hepatotoxicity associated with high intravenous regimens.[10,18,20]

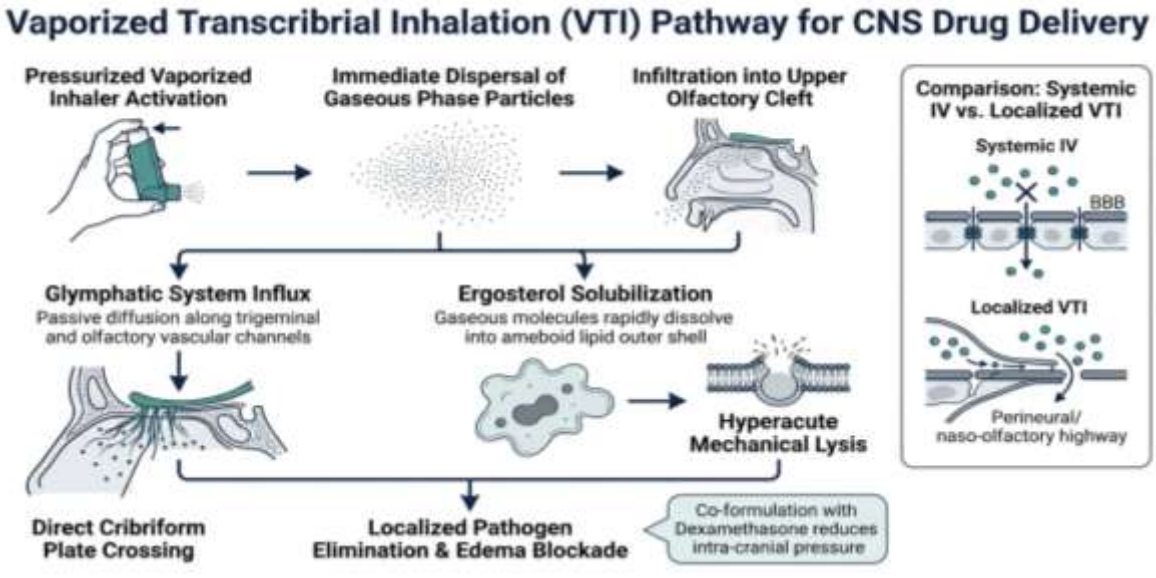

Figure 8: Non-invasive olfactory delivery route for hybrid nano-biologics (Created in Scispace (https://Scispace.com))

Biophysical models have shown that active payloads delivered in vapour phase are substantially more antimicrobial potent than active payloads delivered in conventional liquid formulations. Comparative phase tracking shows that active agents in gaseous state are more efficiently dissolved in the hydrophobic, ergosterol-rich plasma membrane of *N. fowleri* amoeboid trophozoite.[10] For instance, key volatile compounds require a minimum of only 32.7 mg/L in

the vapour phase to achieve 100% cidal effects on cell membranes, compared to a significantly higher requirement of 288 mg/L in the liquid phase. Exposure to the vapour causes rapid accumulation in the ameboid outer membrane, causing surface deformities and mechanical rupture of the cell.[10] Preferably these vapourised intranasal devices include small-molecule candidates with molecular weights ranging from 219 g/mol to 947 g/mol, which are the preferred physical parameters for absorption across the nasal mucosa. To optimize clinical outcomes, these devices combine multi-targeted co-formulations of a potent fast-acting amoebicide (e.g. miltefosine, staurosporine or core triazoles) with an anti-inflammatory corticosteroid like dexamethasone.[10,20]

This dual-action combination approach creates a powerful clinical synergy: the vaporized antimicrobial halts pathogen progression within the olfactory bulb cleft while the local steroid modulates neuroinflammatory cytokine storms, protects endothelial boundaries and reduces intracranial pressure (ICP) surges to prevent lethal vasogenic edema.[10,20] These pressurized inhalers are easy to use, structurally very stable and are suitable for primary healthcare or post-exposure prophylaxis, providing an effective alternative to high risk neurosurgical procedures such as intrathecal or intraventricular cannulation.[10]

3.7.2: Metallic and Terpene-Nanoconjugate Fusions

The development of hybrid nano-biologics, combining the distinctive physical properties of metallic nanoparticles with the inherent antimicrobial actions of natural terpenes, is a significant advance in anti-protozoal nanomedicine. Natural bicyclic and diterpenoid molecules such as andrographolide, forskolin and borneol possess broad spectrum anti-inflammatory, membrane disruptive and neuroprotective properties but their clinical use is limited by their poor aqueous solubility and high volatility.[9] To overcome these limitations, stable Silver Nanoparticle-Terpene Fusions (Terp-AgNPs) were engineered through a single-step green reduction approach, that utilizes the hydroxyl networks of the native terpenes to reduce silver nitrate precursors without the need of toxic chemical stabilizers.[9]

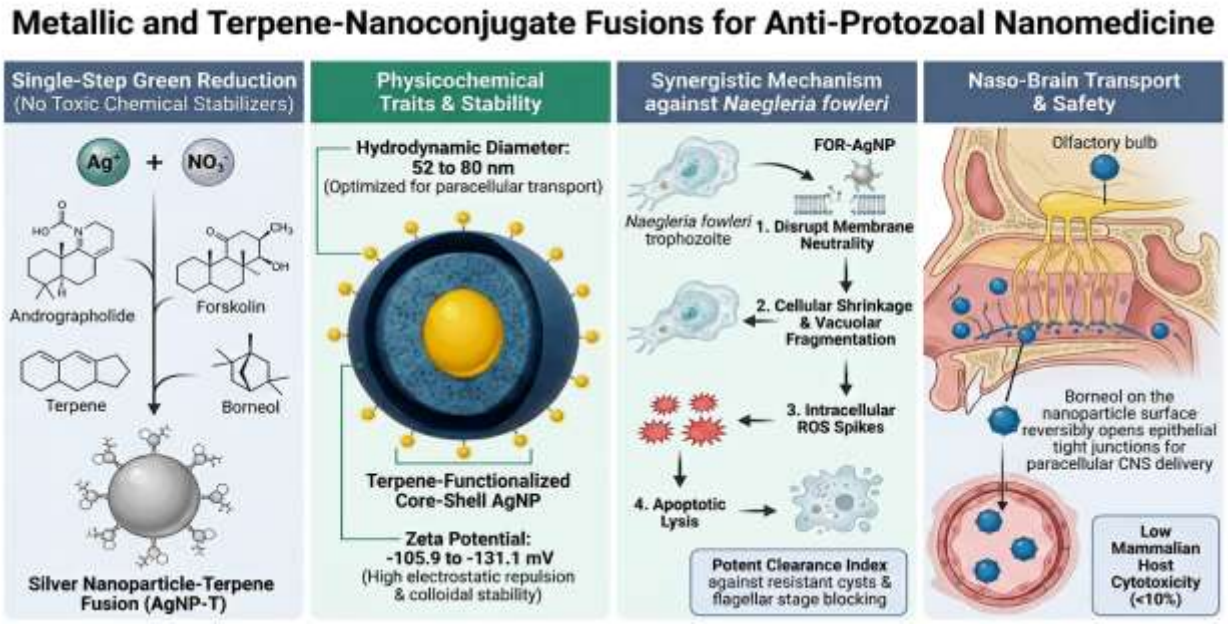

Figure 9; Design, physicochemical characterization, amoebicidal mechanism, and nose-to-brain delivery of metallic-terpene nanoconjugates. (Created in Scispace (https://Scispace.com))

Physicochemical characterization indicates successful nanoconjugation and long-term colloidal stability. Transmission electron microscopy confirms that the synthesized Terp-AgNPs exist as uniform, highly crystalline spherical structures with a narrow hydrodynamic diameter range of 52 to 80 nm, which is optimum for paracellular transport. Zeta potential values ranged between -105.9 and -131.1 mV indicate

a highly negative surface charge distribution, providing strong electrostatic repulsion which prevents particle aggregation over time.[9] Phenotypic whole-cell screening reveals that nano conjugation significantly enhances the direct amoebicidal activity of these terpenes against *Naegleria fowleri* trophozoites, inducing complete proliferation suppression within 24 hours of exposure. The Forskolin-AgNP (FOR-AgNP) fusion produces the most robust direct cidal potency, resolving a low half-maximal inhibitory concentration (IC_{50}) of $26.35 \pm 8.39\ \mu$M against trophozoites and a potent concentration-dependent clearance index ($IC_{50} = 40.90 \pm 3.42\ \mu$M) against resistant cysts, completely inhibiting flagellar and phenotypic life-stage modifications.[9] Mechanistic studies indicated that these terpene nanoconjugates disrupt membrane potential, cause immediate cellular shrinkage, vacuolar fragmentation, and elevated intracellular reactive oxygen species (ROS) levels which lead the pathogen into a rapid apoptotic lysis.[9] Importantly, borneol on the nanoparticle surface acts as an endogenous chemical penetration enhancer, which reversibly opens the tight junctions to enhance the transport across nasal mucosa and cribriform plate. In mammalian cytotoxicity assays, the nanoconjugate maintained host cell damage below 10%, confirming its favourable biocompatibility for intranasal CNS delivery.[9]

CONCLUSION

Comprehensive mapping of advanced pharmacotherapy pipelines, target chokepoints, and novel delivery mechanisms analysed across the definitive scientific literatures provides a clear translational roadmap against Primary Amoebic Meningoencephalitis (PAM). To replace the dependence on toxic slow-acting empirical intravenous cocktails, there must be rapid non-biased screening pipelines targeting highly conserved internal enzyme architectures of *Naegleria fowleri*. Future therapeutic combinations must evaluate candidate molecules by their kinetic onset of action, prioritizing rapid-clearing agents (such as posaconazole and nitroxoline) to halt amoebic trogocytosis at the earliest stage of clinical presentation. Furthermore, for the reason that the hyper-inflammatory immune response within the intracranial space contributes directly to fatal brain herniation, antimicrobial administration must be paired with controlled neuroprotective interventions. A dual intervention of dexamethasone and controlled therapeutic hypothermia is a cornerstone strategy that suppresses microglial inflammatory activity while slowing parasite actin polymerization kinetics to impede neuro-invasion. Ultimately, circumventing the tight junctions of the blood–brain barrier requires shifting from systemic hematogenous routes toward direct trans-cribriform intranasal delivery. Formulating metallic nanoconjugates or multi-epitope mRNA sequences within stimuli-responsive *in-situ* gelling networks offers a targeted, non-invasive delivery platform. By maximizing mucosal retention and accelerating paracellular transport across the cribriform plate, this delivery approach directs therapeutic payloads straight into the olfactory bulb cleft, providing a safe and accessible cure to completely eradicate the threat of brain-eating amoebae.

REFERENCES

1. Maciver SK, Piñero JE, Lorenzo-Morales J. Is Naegleria fowleri an Emerging Parasite? Trends Parasitol. 2020;36(1):19–28. doi:10.1016/j.pt.2019.10.008 PubMed PMID: 31744676.
2. Ahmad Zamzuri M ‘Ammar I, Abd Majid FN, Mihat M, Ibrahim SS, Ismail M, Abd Aziz S, et al. Systematic Review of Brain-Eating Amoeba: A Decade Update. Int J Environ Res Public Health. 2023;20(4):3021. doi:10.3390/ijerph20043021
3. Chen XT, Zhang Q, Wen SY, Chen FF, Zhou CQ. Pathogenic free-living amoebic encephalitis from 48 cases in China: A systematic review. Front Neurol. 2023;14. doi:10.3389/fneur.2023.1100785
4. Asokan S, Choudekar A, V M, Sm R, Abbas RK, Hadi ZS, et al. Amoebic meningoencephalitis in Kerala: Insights for strengthening global health preparedness. Mass Gather Med. 2025; 4:100037. doi: 10.1016/j.mgmed.2025.100037
5. Khurana S. The outbreak of amoebic meningoencephalitis in Kerala: A wake-up call. Indian J Med Res. 2026;162(5):559–62. doi:10.25259/IJMR_2975_2025

6. Chao-Pellicer J, Arberas-Jiménez I, Fuchs F, Sifaoui I, Piñero JE, Lorenzo-Morales J, et al. Repurposing of Nitroxoline as an Alternative Primary Amoebic Meningoencephalitis Treatment. Antibiotics. 2023;12(8):1280. doi:10.3390/antibiotics12081280
7. Sohn HJ, Ham AJ, Park AY, Lee JH, Park S, Shin HJ, et al. Cloning of nf-profilin and intercellular interaction with nf-actin in Naegleria fowleri cysts. Sci Rep. 2025;15(1):7015. doi:10.1038/s41598-025-90222-w
8. Siddiqui R, El-Gamal MI, Boghossian A, Saeed BQ, Oh CH, Abdel-Maksoud MS, et al. Imidazothiazole Derivatives Exhibited Potent Effects against Brain-Eating Amoebae. Antibiotics. 2022;11(11):1515. doi:10.3390/antibiotics11111515
9. Rajendran K, Ahmed U, Meunier AC, Shaikh MF, Siddiqui R, Anwar A. Nanoparticle-Terpene Fusion: A Game-Changer in Combating Primary Amoebic Meningoencephalitis Caused by Naegleria fowleri. ACS Omega. 2024;9(10):11597–607. doi:10.1021/acsomega.3c08844
10. Siddiqui R, Abouleish MY, Khamis M, Ibrahim T, Khan NA. Potential Application of Vaporized Drugs via Nasal Inhalers to Prevent Mortality and Central Nervous System Damage Caused by Primary Amoebic Meningoencephalitis Due to Naegleria fowleri. ACS Pharmacol Transl Sci. 2021;4(3):1249–52. doi:10.1021/acsptsci.1c00086
11. Fong H, Leid ZH, Debnath A. Approaches for Targeting Naegleria fowleri Using Nanoparticles and Artificial Peptides. Pathogens. 2024;13(8):695. doi:10.3390/pathogens13080695
12. Defillo A, Nussbaum E, Parvathy H, Alexander M, S N. Hypothermia as an Adjunctive Treatment in Pediatric Patients with Naegleria fowleri: A Systematic Review. J Pediatr Neurol Neurosci. 2021;5. doi:10.36959/595/417
13. Rice CA, Colon BL, Chen E, Hull MV, Kyle DE. Discovery of repurposing drug candidates for the treatment of diseases caused by pathogenic free-living amoebae. PLoS Negl Trop Dis. 2020;14(9): e0008353. doi: 10.1371/journal.pntd.0008353
14. Rajendran K, Tayo L, Gomez M, Devandran A, Thevanayagam H, Chan SW, et al. Brain-Eating Amoeba Meets Plant Defense: In Vitro and In Silico Evaluation of Malabaricones as Potent Anti-Naegleria fowleri Agents. Prog Microbes Mol Biol. 2025;8. doi:10.36877/pmmb. a0000469
15. Hahn HJ, Debnath A. In Vitro Evaluation of Farnesyltransferase Inhibitor and its Effect in Combination with 3-Hydroxy-3-Methyl-Glutaryl-CoA Reductase Inhibitor against Naegleria fowleri. Pathogens. 2020;9(9):689. doi:10.3390/pathogens9090689
16. Colon BL. Drug discovery and development of resistance in naegleria fowleri identifies potent compounds and novel targets to treat primary amoebic meningoencephalitis [Internet]. University of Georgia; 2018 [cited 2026 Jul 1]. Available from: https://openscholar.uga.edu/record/11536
17. Martín-Escolano R, Yiangou L, Kazana E, Robinson GK, Michaelis M, Tsaousis AD. Repurposing in vitro approaches for screening anti-parasitic drugs against the brain-eating amoeba Naegleria fowleri. Int J Parasitol Drugs Drug Resist. 2021; 17:204–12. doi: 10.1016/j.ijpddr.2021.10.003
18. Siddiqui R, Lloyd D, Khan NA. Emerging patents versus brain eating amoebae, Naegleria fowleri. Pharm Pat Anal. 2024;13(4–6):181–6. doi:10.1080/20468954.2025.2459584 PubMed PMID: 39901763.
19. Chen C wen, Moseman EA. Pro-inflammatory cytokine responses to Naegleria fowleri infection. Front Trop Dis. 2023;3. doi:10.3389/fitd.2022.1082334
20. Siddiqui R, Khan NA. Intranasal Route for the Delivery of Antiamebic Drugs Against brain-eating Amoeba. Ther Deliv. 2023;14(3):175–7. doi:10.4155/tde-2023-0015 PubMed PMID: 37191013.
21. Ferrante A, Rowan-Kelly B. The role of antibody in immunity against experimental naegleria meningoencephalitis ('amoebic meningitis'). Immunology. 1988;64(2):241–4. PubMed PMID: 3391642; PubMed Central PMCID: PMC1384949.
22. Rodríguez-Mera IB, Carrasco-Yépez MM, Vásquez-Moctezuma I, Correa-Basurto J, Salinas GR, Castillo-Ramírez DA, et al. Role of cathepsin B of Naegleria fowleri during primary amebic

meningoencephalitis. Parasitol Res. 2022;121(11):3287–303. doi:10.1007/s00436-022-07660-y

23. Siddiqui R, Boghossian A, Khatoon B, Kawish M, Alharbi AM, Shah MR, et al. Antiamoebic Properties of Metabolites against Naegleria fowleri and Balamuthia mandrillaris. Antibiotics. 2022;11(5):539. doi:10.3390/antibiotics11050539
24. Kyere-Davies G, Agyare C, Boakye Y, Trpta B, Brian M, James H, et al. In vitro activity of selected Ghanaian medicinal plants against parasites: Giardia lamblia, Entamoeba histolytica and Naegleria fowleri. Afr J Pharm Pharmacol. 2017; 11:279–83. doi:10.5897/AJPP2017.4795
25. Arberas-Jiménez I, Rodríguez-Expósito RL, San Nicolás-Hernández D, Chao-Pellicer J, Sifaoui I, Díaz-Marrero AR, et al. Marine Meroterpenoids Isolated from Gongolaria abies-marina Induce Programmed Cell Death in Naegleria fowleri. Pharmaceuticals. 2023;16(7):1010. doi:10.3390/ph16071010
26. Arberas-Jiménez I, Cen-Pacheco F, Chao-Pellicer J, Sifaoui I, Rizo-Liendo A, Morales EQ, et al. Identification and characterization of novel marine oxasqualenoid yucatecone against Naegleria fowleri. Int J Parasitol Drugs Drug Resist. 2023; 22:61–71. doi: 10.1016/j.ijpddr.2023.05.004
27. Naveed M, Ali U, Aziz T, Jabeen K, Arif MH, Alharbi M, et al. Development and immunological evaluation of an mRNA-based vaccine targeting Naegleria fowleri for the treatment of primary amoebic meningoencephalitis. Sci Rep. 2024;14(1):767. doi:10.1038/s41598-023-51127-8
28. Rojas-Hernández S, Rodríguez-Monroy MA, López-Revilla R, Reséndiz-Albor AA, Moreno-Fierros L. Intranasal Coadministration of the Cry1Ac Protoxin with Amoebal Lysates Increases Protection against Naegleria fowleri Meningoencephalitis. Infect Immun. 2004;72(8):4368–75. doi:10.1128/iai.72.8.4368-4375.2004.

Cite: Muhammed Danish Haneefa, Ashik T. N., Aparna E., Jisha Mohanan*, The Evolving Arsenal Against Naegleria Fowleri: From Empirical Poly-Chemotherapy to Target-Driven Repurposing Pipelines, Int. J. Med. Pharm. Sci., 2026, 2 (9), 602-620. https://doi.org/10.5281/zenodo.23008145